

Voltage control for Photo Voltaic Systems with MPPT and Battery Storage in Micro grids

M.R.Prasad¹, V.Sravan Kumar² and P.Srihari³

¹ PG Scholar Department of EEE, Lakireddy Balireddy College of Engineering, Vijayawada, India

^{2,3} Asst. Professor Department of EEE, Lakireddy Balireddy College of Engineering, Vijayawada, India

ABSTRACT

Distributed energy sources (DE) or Distributed generation with power electronics interface are capable of providing reactive power related to ancillary system services. Power generation capability of Photo Voltaic (PV) systems mainly depends on solar irradiance and temperature constraints while these are continuously varying, in order to extract maximum amount of power from PV system maximum power point tracking technique (MPPT) to be employed. In the point of power system reliability and voltage stability local voltage regulation has drawn much more importance. This paper proposes integrated control of voltage at voltage source inverter (VSI) ac side and MPPT algorithm at PV side along with Battery storage control. By these control techniques effective utilization of PV system can be achieved and also voltage stability is improved. Also battery storage supports the PV system while in emergencies.

Key Words: Distributed energy resource (DER), distributed generation (DG), maximum power point tracking (MPPT), voltage control, solar photovoltaic (PV).

1. INTRODUCTION

Distributed generation, also called on-site generation, dispersed generation, embedded generation, decentralized generation, decentralized energy, distributed energy or district energy, generates electricity from many small energy sources. Most countries generate electricity in large centralized facilities, such as fossil fuel (coal, gas powered), nuclear, large solar power plants or hydropower plants. These plants have excellent economies of scale, but usually transmit electricity long distances and can negatively affect the environment. Distributed generation allows collection of energy from many sources and may give lower environmental impacts and improved security of supply.

The micro grid is a collection of distributed generators or Micro resources, energy storage devices, and loads which operate as a single and independent controllable system capable of providing both power and heat to the area of service. The micro resources that are

incorporated in a micro grid are comprised of small units, provided with power electronics (PE) interface. Most common resources are Solar Photovoltaic (PV), Fuel Cell (FC), or micro turbines connected at the distribution voltage level. In a micro grid, the micro sources and storage devices are connected to the feeders through the micro source controllers (MCs) and the coordination among the micro sources is carried out by the central controller (CC). The micro grid is connected to the medium voltage level utility grid at the point of common coupling (PCC) through the circuit breakers.

The operation and control of the inverter interface of renewable- based distributed energy resources (DERs), like Solar Photovoltaic (PV) in a micro grid, is a real challenge, especially when it comes to maintaining both micro grid voltage and frequency within an acceptable range. A voltage control method based on traditional droop control for voltage sag mitigation along with voltage ride through capability is proposed in [1]. A dynamic voltage regulation based on adaptive control is proposed in [2], [3]. In [5], frequency regulation with PV in micro grids is studied; however, this work does not consider the voltage control objective and lacks battery storage in the micro grid. In [8], load frequency control is implemented in micro grid with PV and storage; however, this work also lacks the consideration of a voltage control objective. In summary, the previous works in this topic either lack the incorporation of an energy storage component or the voltage control objective. The present work fulfils these gaps by considering all of these objectives.

This paper proposes several control algorithms through which the capability of PV generators for voltage control and to extract maximum power by MPPT control. Detailed models of PV, battery, inverter and converter are considered for the study. The major contribution and novelty of the proposed control methods lie in the coordination among individual proposed control methods: MPPT control at the PV side, battery control, and Voltage control algorithm at the inverter side. These three control algorithms at three stages are jointly linked through a power balance objective at the DC and AC side of the inverter so that the DC side voltage is indirectly controlled at the desired value in order to maintain the AC side voltage at the utility desired voltage. This is a very important contribution from this work as compared to

other literatures in this area. These parameters can be adaptively achieved with the changing system conditions which could be a very promising future direction of this work. The rest of the paper is organized as follows: Chapter 2 briefly presents the analytical modelling of Solar PV & describes the modelling of the battery storage. Chapter 3 describes the proposed Voltage sag mitigation control while incorporating PV MPPT control and battery storage control. Chapter 4 presents simulation results for proposed system.

2. PROPOSED SYSTEM CONFIGURATION

Fig. 1 shows the PV system configuration for Voltage control while PV operating at MPP including the battery storage backup. It is a two-stage configuration where a DC-DC boost converter is used for MPPT control. The system also considers a battery back-up in case of emergencies while maintaining the voltage of the micro grid or while trying to supply the critical loads.

A battery is connected in parallel to the PV to inject or absorb active power through a bidirectional DC-DC converter. When the battery is absorbing power, the converter operates in the buck mode and when battery is injecting power to the grid, it operates in the boost mode. The operation mode is maintained through the control signal provided to the converter switches.

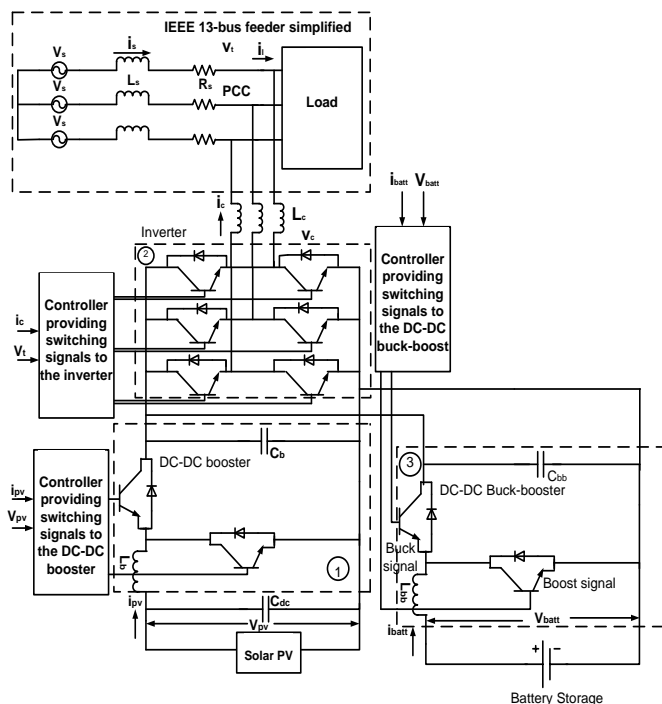


Fig.1. System configuration of V-f control with solar PV generator operating at MPPT with a battery storage system.

The PV system is connected to the grid through a coupling inductor. The coupling inductor filters out the

ripples in the PV output current. The connection point is called the point of common coupling (PCC) and the PCC voltage is denoted as $v_t(t)$. The rest of the system in Fig. 3 denotes the IEEE 13-bus distribution feeder which is simplified as a substation with the feeder equivalent impedance, $R + j\omega L_s$. The details of the IEEE-13 bus system will be described in the next section. The PV source is connected to the DC link of the inverter with a capacitor. The PV is the active power source, and the capacitor is the reactive power source of the PV system.

According to the instantaneous power definitions, for a balanced three-phase system, if and denote the instantaneous PCC voltage and the inverter output voltage (harmonics neglected), respectively, then the average power of the PV denoted as $P(t)$, the apparent power $S(t)$ and the average reactive power $Q(t)$ of the PV are as given below

$$P(t) = \frac{2}{T} \int_{t-\frac{T}{2}}^t v_t(\tau) i_c(\tau) d\tau = \frac{v_t(t)v_c(t)}{\omega L_c} \sin \alpha \quad (1)$$

$$S(t) = V_t(t) I_c(t) = \frac{v_t(t)}{\omega L_c} \sqrt{v_t(t)^2 + v_c(t)^2 - 2v_t(t)v_c(t) \cos \alpha} \quad (2)$$

$$Q(t) = \sqrt{S(t)^2 - P(t)^2} = \frac{v_t(t)}{\omega L_c} (v_c(t) \cos \alpha - v_t(t)) \quad (3)$$

Here, α is the phase angle of $v_c(t)$ relative to the PCC voltage. $P(t)$ and $Q(t)$ in (1) and (3) can be approximated by the first terms of the Taylor series if the angle α is small, as shown in (4) and (5):

$$P(t) \approx \frac{v_t(t)v_c(t)}{\omega L_c} \alpha \quad (4)$$

$$Q(t) \approx \frac{v_t(t)}{\omega L_c} (v_c(t) - v_t(t)) \quad (5)$$

2.1 Solar Pv Modeling

The commonly accepted solar cell model is a one diode model [7]. This work uses the single diode model of the solar cell to model the Kyocera KD240GX-LPB solar array, which is shown in Fig. 2.

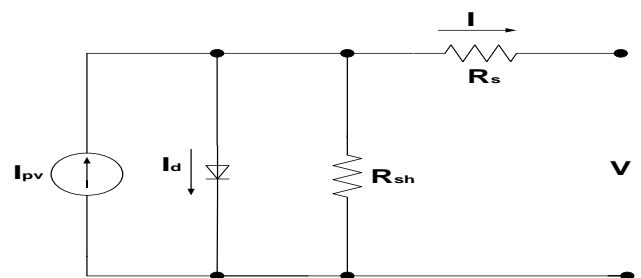


Fig.2. One diode equivalent circuit of solar PV

The I-V characteristics of a solar array, as shown in Fig. 3, are represented by (6).

$$I = I_{pv} - I_o \left[\exp \left(\frac{V + IR_s}{V_{therm} a} \right) - 1 \right] - \frac{V + IR_s}{R_{sh}} \quad (6)$$

Where I_{pv} and I_o are the photo current and the diode saturation currents, respectively; $V_{therm} (= N_s kT/q)$ is the

thermal voltage of the array, N_s being the cells connected in series for greater output voltage, k is the Boltzmann constant ($1.3806503 \times 10^{-23}$ J/K), T (Kelvin) is the temperature of the p-n junction of the diode, and q ($1.60217646 \times 10^{-19}$ C) is the electron charge; R_s and R_{sh} are the equivalent series and shunt resistances of the array, respectively; and a is the ideality factor usually chosen in the range $1 \leq a \leq 1.5$. Here a is taken as 1. The photocurrent of the PV array depends linearly on the solar irradiance and the cell temperature, as shown by (7) [7].

$$I_{PV} = (I_{PV,n} + K_1 \Delta T) \frac{G}{G_n} \quad (7)$$

Where $I_{PV,n}$ is the photocurrent at the standard test condition (STC, 25 C and 1000 W/m^2); k_1 is the short circuit current/temperature coefficient; ΔT is the difference between the actual and nominal temperature in Kelvin; G is the irradiation on the device surface; and G_n is the nominal radiation, both in W/m^2 . $I_{PV,n}$ can be calculated based on (8)

$$I_{PV,n} = \frac{R_{sh} + R_s}{R_{sh}} I_{sc} \quad (8)$$

Using these fundamental equations and parameters from the data sheet, the PV model is developed and verified with the panel datasheet. The parameters of the PV panel under study are shown in Table I.

TABLE 1

 PV Panel Parameters at 1000 W/m^2 and 25°C

Model	Kyocera KD240GX-LPB
P_{MPP}	240 W
V_{MPP}	29.8 V
I_{MPP}	8.06 A
V_{OC}	36.9V
I_{SC}	8.59 A

The PV system under study for the proposed V has 125 strings with each string having 4 series connected panels. The Maximum Power Point (MPP) for a single panel of KD240GX-LPB at 1000 W/m^2 and 25°C (STC) is 240 W. Hence, the maximum power of the PV generator at STC is $125 \times 4 \times 240 = 120 \text{ KW}$. The MPP varies according to the change in irradiance level and cell temperature.

2.4 Battery Modelling

In this paper, the battery model is taken from the MATLAB *SimPowerSystems* library with appropriate parameters which will be used for the proposed controls. The detailed description about the battery model is given in [8]. Due to the intermittent and uncertain nature of solar power output and also the highly fluctuating load demands, deep cycle lead acid batteries are the most common type of battery storage in micro grid applications because the maximum capacity of the battery can be utilized. Hence, in this paper, a battery is modelled as a lead acid battery with appropriate choice of parameters for deep cycle application. It is assumed that the lead acid battery can be discharged up to SOC of 20% and can be charged up to SOC of 80%.

The battery model in [8] is an analytical model with two equations representing the battery discharge and charge models. The battery discharge and charge model for a lead acid battery is given by (9) and (10), respectively

$$V_{Batt} = V_0 - R \cdot i - K \frac{Q}{Q-it} (it + t^*) + Exp(t) \quad (9)$$

$$V_{Batt} = V_0 - R \cdot i - [K \frac{Q}{Q-it}] \cdot it - [K \frac{Q}{it-0.1Q}] i^* + Exp(t) \quad (10)$$

Where V_{batt} is the battery voltage (V), V_0 is the battery constant voltage (V), K is polarisation constant (V/Ah) or polarisation resistance is battery capacity (Ah), Q is battery charge (Ah), Exp is exponential zone amplitude (V), t^* is exponential zone time constant inverse (Ah⁻¹), R is the internal resistance is battery current (A), and i is filtered current (A). In this model, the term for polarisation voltage and polarisation resistance is considered to model the Open Circuit Voltage (OCV) of the battery more accurately. The term inside the first square bracket in (10) represents the polarisation resistance and the second square bracket represents the polarisation voltage.

The size of the battery is selected to provide a maximum backup power to compensate for the PV generation in the case of a very small or no irradiance level. In this work, the MPP of PV generator at STC is 100 kW. Hence, the battery is chosen to provide this amount of power for a maximum of 1 hour with an energy content of 100 kWh. The battery backup is considered for short duration applications like frequency control and supplying power to critical loads in the event of emergency situations. One hour of battery backup is considered to be enough for other backup generators to take over the controls in the micro grid emergency situations.

3. MPPT AND BATTERY INTEGRATED VOLTAGE CONTROL METHODS

Proposed MPPT and Battery integrated voltage controlled solar PV system is presented in Fig.5. The control comprises of one loop for MPPT control, one loop for Voltage control at the inverter side and another loop for battery power management.

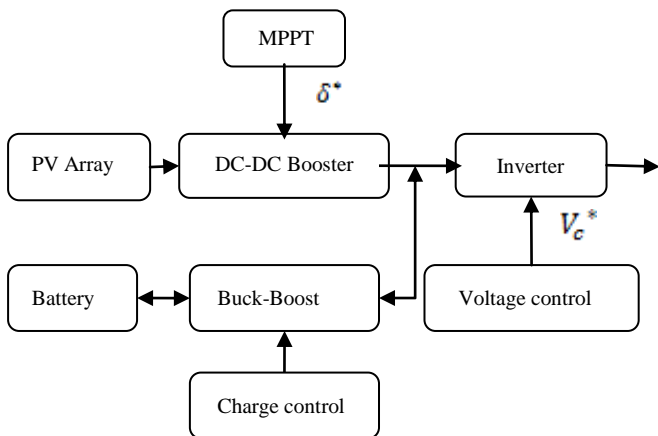


Fig.5. Proposed System Configuration

A typical solar panel converts only 30 to 40 percent of the incident solar irradiation into electrical energy. Maximum power point technique is used to improve the efficiency of the solar panel. According to Maximum Power Transfer theorem, the power output of a circuit is maximum when the Thevenin impedance of the circuit (Source impedance) matches with the load impedance. Hence our problem of tracking the maximum power point reduced to impedance matching problem. In the sources side we are using a boost converter connected to a solar panel in order to enhance the output voltage so that it can be used for different application like motor load. By changing the duty cycle of the boost converter appropriately we can match the source impedance with that of the load impedance.

This chapter describes process of tracking maximum power point which is called Maximum power point tracking. In recent years, a large number of techniques have been proposed for maximum power point tracking (MPPT), such as Incremental conductance method, fractional open circuit voltage, fractional short circuit current, Perturb and Observe (hill-climbing) method. The majority of these methods are based on the perturbation and observation (P&O), which has the advantage of simple operation and easy to implement.

The “P&O” method is that which is most commonly used in practice by the majority of authors. It is an iterative method of obtaining MPP. It measures the PV

array characteristics, and then perturbs the operating point of PV generator to encounter the change direction.

The maximum point is reached when $\frac{dP_{pv}}{dV_{pv}} = 0$. An

example algorithm flowchart of the most basic form is shown in Fig. 6.

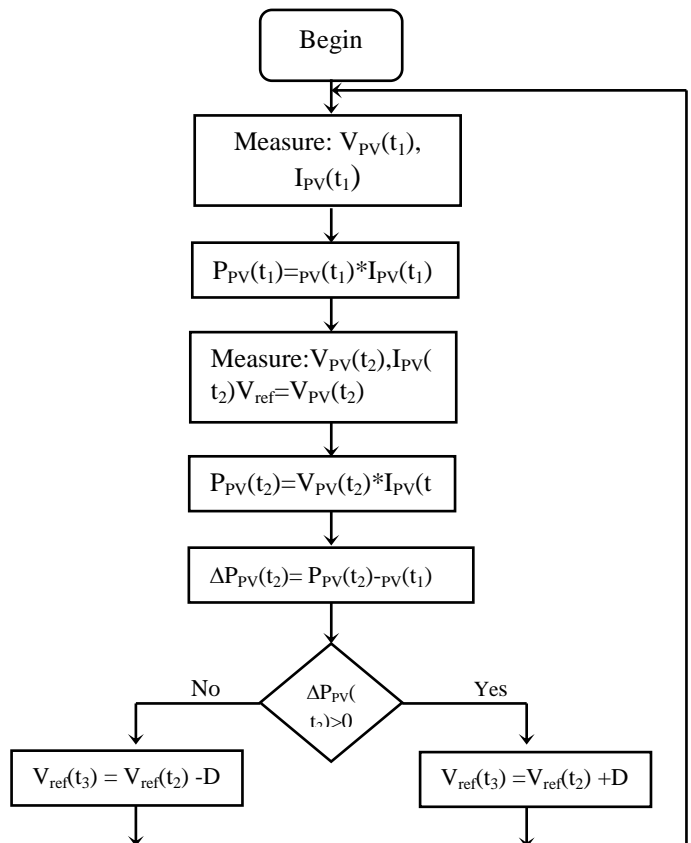


Fig. 6 Conventional P&O algorithm flowchart. D is the step of the perturbation.

Doing this, the operating voltage of the PV generator is perturbed, by a small increment ΔV_{pv} , and the resulting change, ΔP_{pv} , in power, is measured. If ΔP_{pv} is positive, the perturbation of the operating voltage should be in the same direction of the increment. However, if it is negative, the system operating point obtained moves away from the MPPT and the operating voltage should be in the opposite direction of the increment. The logic of this algorithm is explained in Table 2.1 and Fig. 6. True table associated with the operation for the Perturbation and Observe (P&O) method.

Table 2.1: Operation of P&O algorithm

$\Delta P_{pv}(t_2)$	$V_{pv}(t_3)$
>0	+

<0	-
----	---

The “+” sign refers to an increment and “-” sign to a decrease. In accordance with Table 2.1, if the PV power has increased, the operating point should be increased as well. However, if the PV power has decreased, the voltage should do the same.

Nevertheless, a disadvantage of this method appears in the case of a sudden increase of irradiance, Fig. 7. Where the algorithm reacts as if the increase occurred as a result of the previous perturbation of the operating voltage. In order to better understand this phenomenon, see Fig. 7. Thus, the case is considered in which the irradiance is such that it generates the P-V curve characteristics, curve 1. In this way, the operating voltage initially oscillates around the maximum point, from A to A1. Now, an increase in the power will be measured because the solar irradiation has increased from curve 1 to curve 2. Then, if one assumes that being in point A, that it comes from a diminution of the voltage, and before the following disturbance takes place, the irradiance is increased, with the curve characteristic being now curve 2, and the operation point will occur at B1. Indeed, since there has been a positive increase in power, the disturbance will continue in the same direction, see Table 2.1.

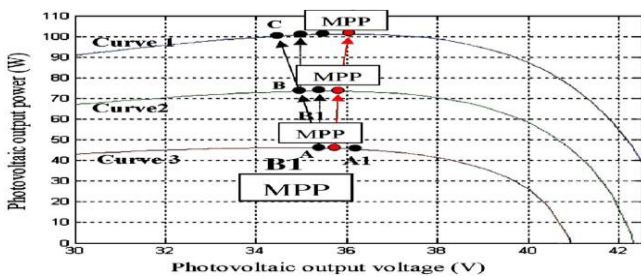


Fig. 7 Deviation from the MPP with the P&O algorithm under rapidly changing

In other words, the voltage will diminish and go to point B. Furthermore, if the irradiance is increased again quickly to curve 3, there will be another increase in positive power, with which the operation point will now be C. That is, due to two increases of irradiance, the operation point has been transferred from A to C, moving away from the maximum point. This process remains until the increase of the irradiance slows or stops.

The advantages of this method can be summarized as follows: a previous knowledge is not required of PV generator characteristics; it a relatively simple method. Nevertheless, in their most simple form, at a steady state, the operating point oscillates around the MPP, giving rise to the wasting of some amount of available energy.

Second loop consists of Voltage control at AC side of the inverter. As shown in the control diagram in Fig. 8 (loop2), the PCC voltage is measured and the rms value of is calculated. Then, the rms value $v_t(t)$ is compared to a voltage reference $v_t^*(t)$ which could be a voltage specified by the utility, and the error is fed to a PI controller. The inverter output voltage $v_c^*(t)$ is controlled so that it is in phase with the PCC voltage, and the magnitude of the inverter output voltage is controlled so that the PCC voltage is regulated at a given level $v_t^*(t)$. The control scheme can be specifically expressed as (11).

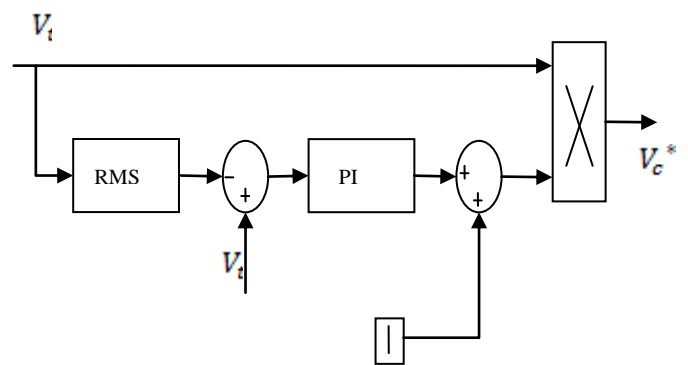


Fig.8. Integrated Solar PV MPPT and V-f control diagram

$$v_{c1}^*(t) = [1 + K_{p2}(v_t^*(t) - v_t(t)) + K_{I2} \int_0^t (v_t^*(t) - v_t(t) dt)] v_{tt}$$

(11) Where K_{p2} and K_{I2} are the controller gains for this loop. In (11), 1 has been added to the right-hand side such that when there is no injection from the PV generator, the PV output voltage is exactly the same as the terminal voltage.

The controls shown in the diagram of Fig. 5 and described above are also integrated with the battery power control shown in Fig. 9. The battery is incorporated in the PV system configuration in order to supply or absorb active power and support the frequency control objective with the PV generator.

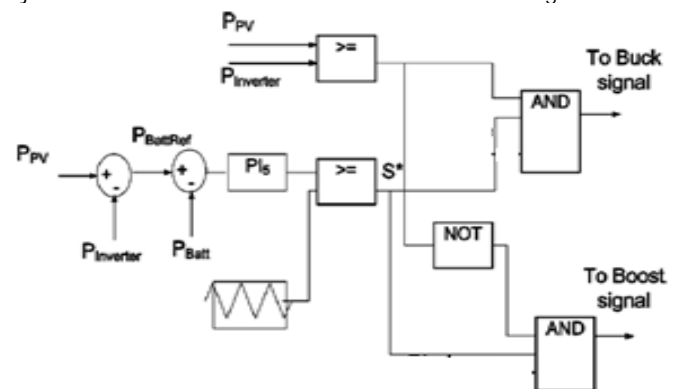


Fig.9. Battery power control diagram

If there is abundant solar power and the active power required for frequency control is less than PV MPP, then

the battery will be charged. If there is not enough solar power available and if the active power required for frequency control is more than PV MPP, then the battery will supply the deficit power in order to maintain the micro grid frequency at 50 Hz. Hence, the control methods for the battery charge/discharge that depends on this requirement, which is developed as shown in the Figure.9.

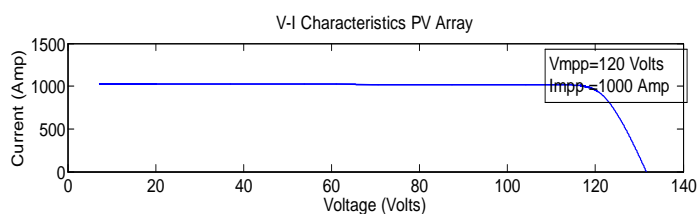
In Fig. 9, the reference power to the battery, $P_{Battref}$ is generated dynamically by subtracting the inverter active power injection, $P_{inverter}$ from the power generated by PV, P_{PV} . The controller comprised of a PI controller, P_{I5} which receives the error signal obtained after subtracting the actual battery power, P_{batt} from the battery reference, $P_{Battref}$. The signal obtained from P_{I5} is then compared with a triangular waveform of unity magnitude to generate the signal, S^* . This is similar to common Pulse Width Modulation (PWM) in inverter controls. K_{p5} and K_{i5} are the proportional and integral gains respectively. The equation for this control is given by (12)

$$S^* = K_{p5}(P_{Battref} - P_{Batt}) + K_{i5} \int_0^t (P_{Battref} - P_{Batt}) dt \quad (12)$$

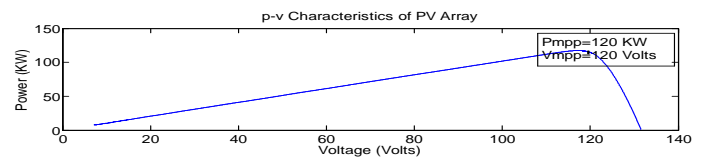
One more step is considered to differentiate the charging and discharging mode of the battery. This is undertaken by comparing P_{PV} with $P_{inverter}$. If $P_{PV} > P_{inverter}$, the battery is in charging mode, hence, the signal obtained from the PWM, S^* and the result of this comparison is passed through a logical AND to generate a switching signal which activates the Buck mode of the DC-DC converter. If the condition is false, (i.e. $P_{PV} < P_{inverter}$), the opposite of this signal and is passed through a logical AND to generate a switching signal which activates the Boost mode of the DC-DC converter. Hence, with this control logic, the converter is capable of operating in both directions and therefore, effectively charging and discharging the battery whenever required.

4. SIMULATION RESULTS AND DISCUSSIONS

A 120 KW PV array is modelled mathematically and simulated at irradiance 1000 W/sq-metre and temperature of 25°C based on Kyocera KC200GT solar array. Fig. a & b shows v-i & v-p characteristic curves PV array

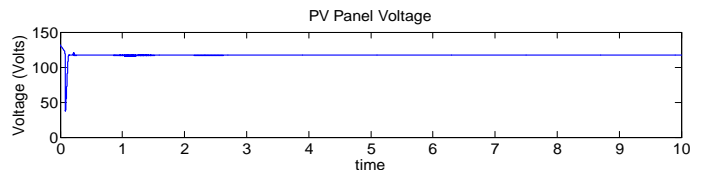


a

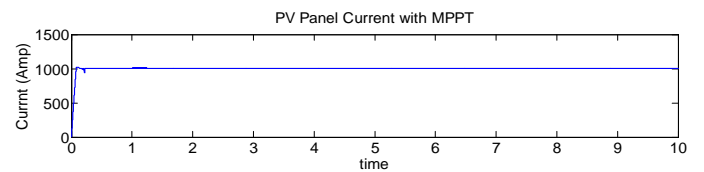


b

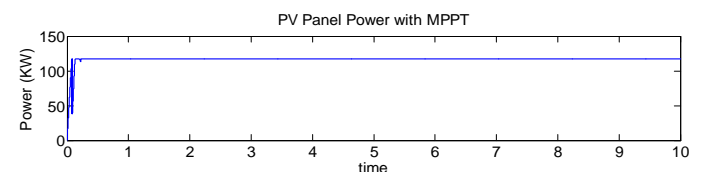
Fig.c,d&e shows the PV array operated maximum values of voltage ,current & power with the help of proposed MPPT technique. maximum power extracted is 120 KW at STC.



c

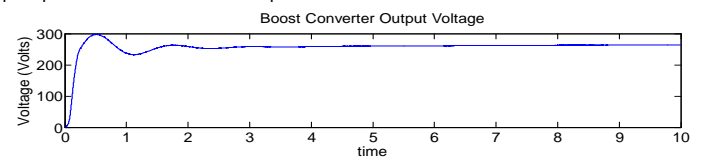


d

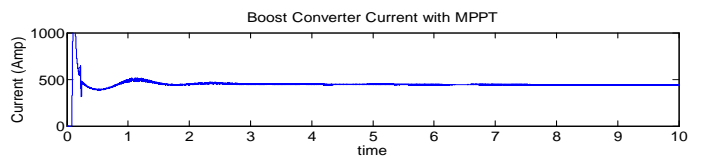


e

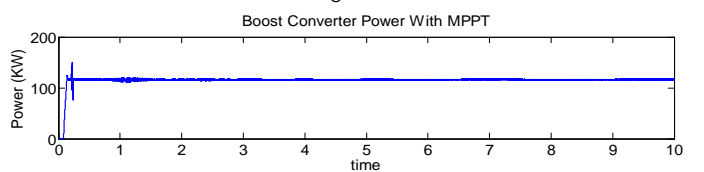
Fig.f,g&h shows maximum values of voltage ,current & power of boost converter stage with the help of proposed MPPT technique.



f



g



h

Fig.i&j shows that PV array generated 120 KW power is shared 35 KW to the inverter and 85 KW battery storage

based on demand. In battery power (-) sign indicates charging of battery.

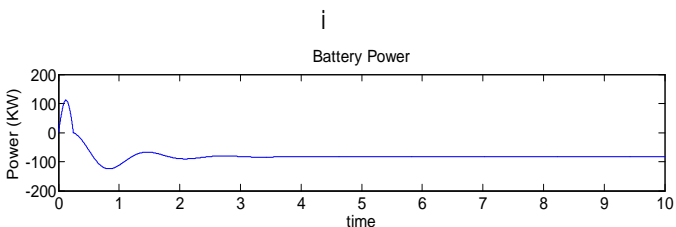
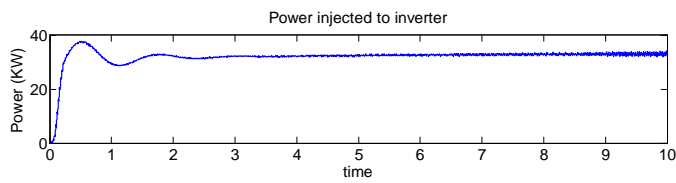
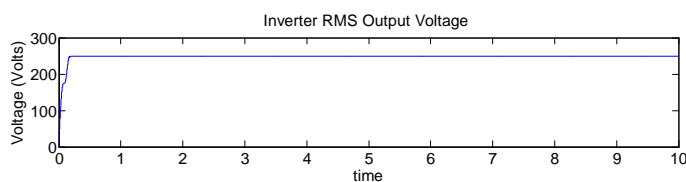


Fig.k. shows the effectiveness of proposed voltage control technique ie. Voltage of the system maintained at 250 V RMS.



5. CONCLUSION

Simulation results show the effectiveness of proposed control techniques for MPPT and Voltage regulation along with battery storage control for Solar PV system. This work can be further extended by implementing frequency support in Islanding mode and P-Q control support in grid connected mode with the help of integrated battery storage control.

REFERENCES

[1] J. C. Vasquez, R. A. Mastromauro, J. M. Guerrero, and M. Liserre, "Voltage support provided by a droop-controlled multifunctional inverter," *IEEE Trans. Ind. Electron.*, vol. 56, pp. 4510–4519, 2009.

[2] H. Li, F. Li, Y. Xu, D. T. Rizy, and J. D. Kueck, "Adaptive voltage control with distributed energy resources: Algorithm, theoretical analysis, simulation and field test verification," *IEEE Trans. Power Syst.*, vol. 25, pp. 1638–1647, Aug. 2010.

[3] H. Li, F. Li, Y. Xu, D. T. Rizy, and S. Adhikari, "Autonomous and adaptive voltage control using multiple distributed energy resources," *IEEE Trans. Power Syst.*, vol. 28, no. 2, pp. 718–730, May 2013.

[4] M. G. Molina and P. E. Mercado, "Modeling and control of grid-connected photovoltaic energy conversion system used as a dispersed generator," in *Proc. 2008 IEEE/PES Transm. Distrib. Conf. Expo.: Latin America*, pp. 1–8.

[5] N. Kakimoto, S. Takayama, H. Satoh, and K. Nakamura, "Power modulation of photovoltaic generator for frequency control of power system," *IEEE Trans. Energy Conv.*, vol. 24, pp. 943–949, 2009.

[6] L. Xu, Z. Miao, and L. Fan, "Coordinated control of a solar battery system in amicrogrid," in *Proc. 2012 IEEE/PES Transm. Distrib. Conf. Expo. (T&D)*, pp. 1–7.

[7] M. G. Villalva, J. R. Gazoli, and E. R. Filho, "Comprehensive approach to modeling and simulation of photovoltaic arrays," *IEEE Trans. Power Electron.*, vol. 24, no. 5, pp. 1198–1208, 2009.

[8] O. Tremblay and L. A. Dessaint, "Experimental validation of a battery dynamic model for EV applications," *World Electric Vehicle J.*, vol. 3, 2009.



M.R.Prasad received B.Tech degree in Electrical and Electronics Engineering from Gokul institute of Technology and Sciences, Bobbili, Andhra Pradesh, India in 2011 and currently He is pursuing M.Tech in lakireddy bali reddy college of engineering, Vijayawada, Andhra Pradesh, India. His areas of interests are Distributed Energy Systems and power flow in microgrids



V.Sravan Kumar received B.Tech degree in Electrical and Electronics Engineering from Koneru Lakshmaiah College of Engineering, Guntur, Andhra Pradesh, India in 2009 and the M.Tech degree in Power Electronics from National Institute of Technology Tiruchy, Tamilnadu, India in 2011. He is currently working as assistant professor in lakireddy bali reddy college of engineering, since June 2011. His areas of interests are Renewable Energy Systems.



P.Srihari received B.Tech degree in Electrical and Electronics Engineering from Nimra College of Engineering, Andhra Pradesh, India in 2008 and the M.Tech degree in Power Systems from V R Siddhartha Engineering College, Vijayawada, Andhra Pradesh, India in 2012. He is currently working as as assistant professor in lakireddy bali reddy college of engineering, since July, 2012. His areas of interests are Renewable Energy Systems.